

QUASI-FLOW CORNER THEORY ON LARGE PLASTIC DEFORMATION OF DUCTILE METALS AND ITS APPLICATIONS*

Hu Ping (胡平)¹ Liu Yuqi (柳玉启)¹

Guo Wei (郭威)¹ Tai Feng (台风)¹

(Received Feb. 24, 1995; Communicated by Chen Dapeng)

Abstract

A quasi-flow corner theory on large plastic deformation of ductile metals is proposed in this paper. From orthogonal rule of plastic flow, the theory introduces a "modulus reduced function" and a corner effect of yield surface into the constitutive model of elastic-plastic large deformation. Thereby, the smooth and continuous transitions from orthogonal constitutive model to non-orthogonal one, and from plastic loading to elastic unloading are realized. In addition, the theory makes it possible to connect general anisotropic yield functions with corner hardening effect. The comparison between numerical simulation and experimental observation for the uniaxial tensile instability and shear band deformation of anisotropic sheet metals shows the validity of the present quasi-flow corner theory.

Key words quasi-flow corner theory, modulus-reduced function, shear band, anisotropy

I. Introduction

In recent decades, the strain localization phenomenon occurring in plastic forming processes of metals has received considerable attention. Numerical simulation results have shown that the localization phenomenon is very sensitive to constitutive model used. To tensile necking and shear fracture of sheet metals, the simulating results obtained from J_2 D theory, which is considered to be short of theoretical foundation of deduction^[1], do show more consistent with experimental ones than that obtained from classical flow theory (J_2 F). This special results have led to the study of non-orthogonal constitutive theories. Stören and Rice^[2] proposed the J_2 deformation theory (J_2 D); Christofferson and Hutchinson^[3] proposed a J_2 corner theory (J_2 C) based on corner effect of yield surface; Gotoh^[4] presented a J_2 G theory from the viewpoint of tensor algebra. However, the same feature of these J_2 class of constitutive theories is that they obey non-orthogonal stress-strain relationship throughout the whole deformation process from initial plastic flow up to deformation instability and fracture. Therefore, an important fact is that these theories neglect physical property of smooth yield surface at initial plastic deformation stage due to pay their attention to the strain localization process after material instability.

* Project supported by the National Distinguished Young Scientist Foundation of China

¹ Jilin University of Technology, Changchun 130025, P. R. China

In the present paper, we propose a quasi-flow corner theory suitable for large deformation instability and fracture analyses, by introducing quasi-elastic modulus evolution function into elastic constitutive tensor and by using anisotropic yield criterion and corner effect on subsequent yield surface. The principal purpose in the present theory is to bring about smooth and continuous transition of the quasi-flow corner theory from the flow theory based on orthogonal rule to the corner theories based on non-orthogonal rule, and from plasticity loading to elasticity unloading; furthermore, to combine 2D smooth anisotropic yield function with corner hardening in order to more reasonably simulate the whole process of large deformation tensile instability and strain localization of anisotropic sheet metals.

II. Quasi-Flow Corner Theory

For most of the metal materials with property of small elastic and large plastic deformations, the total logarithmic strain rate $\dot{\varepsilon}_{ij}$ is assumed to be the sum of the quasi-elastic logarithmic strain rate $\dot{\varepsilon}_{ij}^e$ and the quasi-plastic logarithmic strain rate $\dot{\varepsilon}_{ij}^p$,

$$\dot{\varepsilon}_{ij} = \dot{\varepsilon}_{ij}^e + \dot{\varepsilon}_{ij}^p \quad (2.1)$$

due to the convexity of loading yield surface. According to Ref. [5], $\dot{\varepsilon}_{ij}^e$ obey the following relation

$$\dot{\varepsilon}_{ij}^e = \frac{1}{E_c} \left[\frac{1}{2} (1 + \mu_c) (\delta_{ik} \delta_{jl} + \delta_{il} \delta_{jk}) - \mu_c \delta_{ij} \delta_{kl} \right] \dot{\sigma}_{kl} \quad (2.2)$$

where the quasi-elasticity modulus E_c can generally expressed as a reduced function of the Young's modulus E ,

$$E_c = E \cdot \left[\frac{1}{2} (1 + E_s/E) - \frac{1}{\pi} (1 - E_s/E) \tan^{-1} \left(\frac{\bar{\varepsilon} - \varepsilon^*}{\alpha_0} \right) \right] \quad (2.3)$$

the quasi Poisson's ratio μ_c in Eq. (2.2) is assumed to satisfy volume deformation rule, and expressed as

$$\mu_c = \frac{1}{2} - \frac{E_c}{E} \left(\frac{1}{2} - \mu \right) \quad (2.4)$$

where μ is true Poisson's ratio; E_s is the secant modulus of Kirchhoff stress-logarithmic strain ($\sigma - \varepsilon$) curve on uniaxial tensile condition; $\bar{\varepsilon}$ is the effective strain measured at present deformation state, ε^* is, indeed, a constant relation to material property and deformation patterns; α_0 is a small constant. The modulus reduced function E_c in Eq. (2.3) can describe the smooth evolution of Young's modulus E to secant modulus E_s as plastic deformation develops.

From orthogonal rule and so-called "consistent condition", $\dot{\varepsilon}_{ij}^p$ in Eq. (2.1) can be solved and expressed as^[5]

$$\dot{\varepsilon}_{ij}^p = \left(\frac{\bar{\sigma}}{Mf} \right)^2 \left[\frac{1}{E_t} - \frac{1}{E_c} \right] \frac{\partial f}{\partial \sigma_{ij}} - \frac{\partial f}{\partial \sigma_{kl}} \dot{\sigma}_{kl} = \bar{C}_{ijkl}^p \dot{\sigma}_{kl} \quad (2.5)$$

where f is M -order homogeneous yield function of Cauchy stress σ_{ij} , E_t is tangent modulus of the $\sigma - \varepsilon$ curve.

Using the following identity

$$\frac{1 + \mu_c}{E_c} = \frac{1 + \mu}{E} + \frac{3}{2} \left(\frac{1}{E_c} - \frac{1}{E} \right) \quad (2.6)$$

and assuming

$$I_{ijkl} = \frac{1}{2} (\delta_{ik}\delta_{jl} + \delta_{il}\delta_{jk}) - \frac{1}{3} \delta_{ij}\delta_{kl} \quad (2.7)$$

Eq. (2.1), (2.2) and (2.5) can be concentrated into

$$\begin{aligned} \dot{\epsilon}_{ij} = & \frac{1}{E} \left[\frac{1}{2} (1 + \mu) (\delta_{ik}\delta_{jl} + \delta_{il}\delta_{jk}) - \mu \delta_{ij}\delta_{kl} \right] \tilde{\sigma}_{kl} \\ & + \left[\frac{3}{2} \left(\frac{1}{E_c} - \frac{1}{E} \right) I_{ijkl} + \left(\frac{\tilde{\sigma}}{Mf} \right)^2 \left(\frac{1}{E_i} - \frac{1}{E_c} \right) \frac{\partial f}{\partial \sigma_{ij}} \frac{\partial f}{\partial \sigma_{kl}} \right] \tilde{\sigma}_{kl} \\ = & (B_{ijkl}^e + B_{ijkl}^p) \tilde{\sigma}_{kl} \end{aligned} \quad (2.8)$$

It is easily known that B_{ijkl}^e are true elasticity compliance; therefore, true plastic logarithmic strain rate $\dot{\epsilon}_{ij}^p$ should be

$$\dot{\epsilon}_{ij}^p = B_{ijkl}^p \tilde{\sigma}_{kl} \quad (2.9)$$

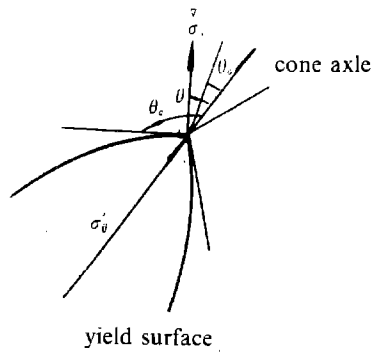


Fig. 1 Corner effect of yield surface

Now, we consider the micro-slipping mechanism of material instability^[6], and assume that corner effect begins occurring at the loading point of yield surface when plastic deformation reaches an extent, and the corner effect gradually becomes sharp as plastic deformation develops. Let θ be the angle between $\tilde{\sigma}_{ij}$ and σ'_{ij} (see Fig. 1), where σ'_{ij} is Cauchy deviatoric stress, the angles θ_0 and θ_c in Fig. 1 divide the loading and unloading ranges at the loading

corner of yield surface into three ranges: $0^\circ \leq \theta \leq \theta_0$ is full loading range; $\theta > \theta_c$ is elastic unloading range and $\theta_0 \leq \theta \leq \theta_c$ is partly unloaded range. In this range, the increment of plastic strain rate will gradually become slow until elastic unloading occurs. To keep the continuous transition, an angle function $\rho(\theta)$ between $\tilde{\sigma}_{ij}$ and σ'_{ij} is introduced in terms of Ref. [3]

$$\rho(\theta) = \begin{cases} 1 & 0 \leq \theta \leq \theta_0 \text{ (full plastic loading)} \\ \cos \left[\frac{\pi}{2} \left(\frac{\theta - \theta_0}{\theta_c - \theta_0} \right) \right] & \theta_0 \leq \theta \leq \theta_c \text{ (partly plastic loading)} \\ 0 & \theta_c \leq \theta \leq \pi \text{ (elastic unloading)} \end{cases} \quad (2.10)$$

The plasticity potential energy W_p at the loading corner is written using quadratic homogeneous formula

$$W_p = \frac{1}{2} \rho(\theta) B_{ijkl}^p \tilde{\sigma}_{ij} \tilde{\sigma}_{kl} \quad (2.11)$$

Total stress rate potential energy function is

$$W = \frac{1}{2} B_{ijkl}^e \tilde{\sigma}_{ij} \tilde{\sigma}_{kl} + \frac{1}{2} \rho(\theta) B_{ijkl}^p \tilde{\sigma}_{ij} \tilde{\sigma}_{kl} = W_e + W_p \quad (2.12)$$

while total logarithmic strain rate tensor can be written as

$$\dot{\epsilon}_{ij} = \frac{\partial^2 W}{\partial \bar{\sigma}_{ij} \partial \bar{\sigma}_{kl}} \bar{\sigma}_{kl} = B_{ijkl}(\theta) \bar{\sigma}_{kl} \quad (2.13)$$

Assuming that

$$\lambda_{ij} = \gamma \sigma'_{ij} \quad (2.14)$$

$$M_{ij} = B_{ijkl}^p \lambda_{kl} \quad (2.15)$$

and normalizing λ_{ij} by using B_{ijkl}^p (i. e. assuming $\lambda_{ij} M_{ij} = 1$), we can solve γ and obtain

$$\lambda_{ij} = (B_{ijkl}^p \sigma'_{ij} \sigma'_{kl})^{-\frac{1}{2}} \sigma'_{ij} \quad (2.16)$$

So, the definition of $\cos\theta$ provides the following expression^[3]

$$\cos\theta = \frac{B_{ijkl}^p \lambda_{ij} \bar{\sigma}_{kl}}{(B_{mnpq}^p \bar{\sigma}_{mn} \bar{\sigma}_{pq})^{\frac{1}{2}}} = \frac{M_{ij} \bar{\sigma}_{ij}}{(B_{mnpq}^p \bar{\sigma}_{mn} \bar{\sigma}_{pq})^{\frac{1}{2}}} \quad (2.17)$$

Using Eqs. (2.8)–(2.10) and (2.13)–(2.17), the plastic logarithmic strain rate determining present loading corner is obtained

$$\dot{\epsilon}_{ij}^p = [\alpha(\theta) B_{ijkl}^p + \beta(\theta) M_{ij} M_{kl}] \bar{\sigma}_{kl} = \bar{B}_{ijkl}^p(\theta) \bar{\sigma}_{kl} \quad (2.18)$$

in which

$$\left. \begin{aligned} \alpha(\theta) &= \rho(\theta) [1 - \kappa(\theta) \cot\theta] \\ \beta(\theta) &= \rho(\theta) \kappa(\theta) (\sin\theta \cdot \cos\theta)^{-1} \\ \kappa(\theta) &= -\frac{1}{2} \rho'(\theta) / \rho(\theta) \end{aligned} \right\} \quad (2.19)$$

It is easily found that when $\sigma'_{ij} // \bar{\sigma}_{ij}$ (corresponding to smooth yield surface), $\theta = 0^\circ$. Thus, $\rho(\theta) = 1$, $\kappa(\theta) = 0$, $\alpha(\theta) = 1$ and $\beta(\theta) = 0$. In this moment, Eq. (2.18) comes back to Eq. (2.9) corresponding to full loading. On the other hand, when $\rho(\theta) = 0$ (corresponding to elasticity unloading), Eq. (2.18) will automatically give $\dot{\epsilon}_{ij}^p = 0$. Therefore, the constitutive equation of quasi-flow corner theory suitable for any yield function can be generally written as

$$\dot{\epsilon}_{ij} = [B_{ijkl}^e + \bar{B}_{ijkl}^p(\theta)] \bar{\sigma}_{kl} \quad (2.20)$$

For isotropic hardening Mises yield function, the B_{ijkl}^p in Eq. (2.9) can be written as

$$B_{ijkl}^p = \frac{3}{2} \left[\left(\frac{1}{E_s} - \frac{1}{E} \right) I_{ijkl} + \frac{3}{2} \left(\frac{1}{E_s} - \frac{1}{E} \right) \frac{\sigma'_{ij} \sigma'_{kl}}{\bar{\sigma}^2} \right] \quad (2.21)$$

Noting that

$$\bar{\sigma}^2 = \frac{3}{2} I_{ijkl} \sigma'_{ij} \sigma'_{kl}, \quad \bar{\sigma}'_{ij} \bar{\sigma}'_{kl} = I_{ijkl} \bar{\sigma}_{ij} \bar{\sigma}_{kl} \quad (2.22)$$

We can obtain

$$\lambda_{ij} = \left(\frac{1}{E_s} - \frac{1}{E} \right)^{-\frac{1}{2}} \frac{\sigma'_{ij}}{\bar{\sigma}}, \quad M_{ij} = \frac{3}{2} \left(\frac{1}{E_s} - \frac{1}{E} \right)^{\frac{1}{2}} \frac{\sigma'_{ij}}{\bar{\sigma}} \quad (2.23)$$

If $\bar{\sigma}$ is assumed as the Jaumann rate of Cauchy effective stress $\dot{\bar{\sigma}}$, we have

$$\ddot{\sigma} = \dot{\sigma} = \frac{3}{2} \frac{1}{\dot{\sigma}} \sigma'_{ij} \ddot{\sigma}_{ij} \quad (2.24)$$

Therefore, Eq. (2.17) is simplified as

$$\cos\theta = \frac{\left(\frac{1}{E_t} - \frac{1}{E}\right)^{\frac{1}{2}} \dot{\sigma}}{\left[\frac{3}{2} \left(\frac{1}{E_c} - \frac{1}{E}\right) \ddot{\sigma}'_{ij} \ddot{\sigma}'_{ij} + \left(\frac{1}{E_t} - \frac{1}{E_c}\right) \dot{\sigma}^2\right]^{\frac{1}{2}}} \quad (2.25)$$

From Eq. (2.3), it can be found that when $\bar{\varepsilon} \ll \bar{\varepsilon}^*$, $E_c \rightarrow E$, and $\theta \rightarrow 0$, which implies that $\ddot{\sigma}_{ij}$ are parallel to σ'_{ij} at initial plastic deformation stage. As plastic deformation develops, E_c will gradually deviate E and trend to secant modulus E_s ; Quasi-flow corner theory mentioned above will gradually evolve to J₂C theory in Ref. [3].

It must be mentioned that in accordance with the angle definition in Ref. [3], σ'_{ij} can not be parallel to $\ddot{\sigma}_{ij}$ at the beginning of plastic deformation. As a consequence, the corner effect of yield surface runs through the whole process from initial plastic deformation up to material instability and fracture. So far as the initial stage of plastic deformation is concerned, the J₂C theory does not obey the orthogonal law of plastic flow. Therefore, the theory deviates from the phenomenological constitutive theories consisting with smooth yield surface, and from the micro-physical theories corresponding to the plastic deformation induced by dislocation slip. On the other hand, own to the continuous evolution of the quasi-elasticity modulus E_c , the present quasi-flow corner theory accomplishes the smooth transition from the flow theory obeying orthogonal law of initial plastic deformation to the J₂ corner theory obeying non-orthogonal law, and keeps the transitional continuity from plastic loading to elastic unloading after plastic instability occurs.

It is easy to know that when $E_c \equiv E$, the present theory returns to the classical flow theory, i. e., Prandtl-Reuss theory. For Mises materials, when $E_c \equiv E_s$, the present theory will come back to J₂C theory in Ref. [3]. It must be mentioned that on disproportional loading condition, calculation results obtained from these theories are obviously different^[6].

III. Numerical Tests

In this section, the quasi-flow corner theory, the planar anisotropic yield function in Ref. [8] are introduced into updating Lagrange finite element formulation^[7] in order to numerically simulate the uniaxial tensile instability and strain localization process of three kinds of planar anisotropic sheet metals. The simulating results are compared with experimental ones in order to examine the validity of the present theory.

(1) Experiment

Taking D15 type low selenium steel thin sheet made in China (specimen I), 08Al sheet (specimen II) and 1Cr18Ni9Ti stainless steel sheet (specimen III), we roll the above sheet metals into normal specimens and set gauge length (width/height=0.4). Then we select five of every type specimen as a group to measure the experimental parameters of uniaxial tension in order to guarantee the statistical reliability of the measured parameters. The statistical averages of the measured material parameters for the three specimens are listed in Table 1.

Now taking five of every normal specimen, we again make on experiment of tensile fracture (along 90 degree rolling direction). The fracture configurations of three kinds of

Table 1 Material parameters of specimens

	R_0	R_{45}	R_{90}	thickness h_0 (mm)	elasticity modulus E (MPa)	strain hardening exponent n	material character
specimen I	0.311	0.517	0.424	0.42	194330	0.168	bcc polycrystal
specimen II	1.961	1.204	2.176	1.80	201000	0.243	bcc polycrystal
specimen III	0.9351	1.5439	1.067	0.84	202000	0.40	fcc polycrystal

in which R_0 , R_{45} and R_{90} are the anisotropic parameters measured along 0, 45 and 90 degrees relating to the rolling direction, respectively.

specimens after tensile fracture occurs are shown in Fig. 2 (a)–(c). The largest stretching and necking ratios in the end of these specimens measured at fracture time are 0.20, 0.42, 0.52 and 0.0642, 0.351, 0.263, respectively.

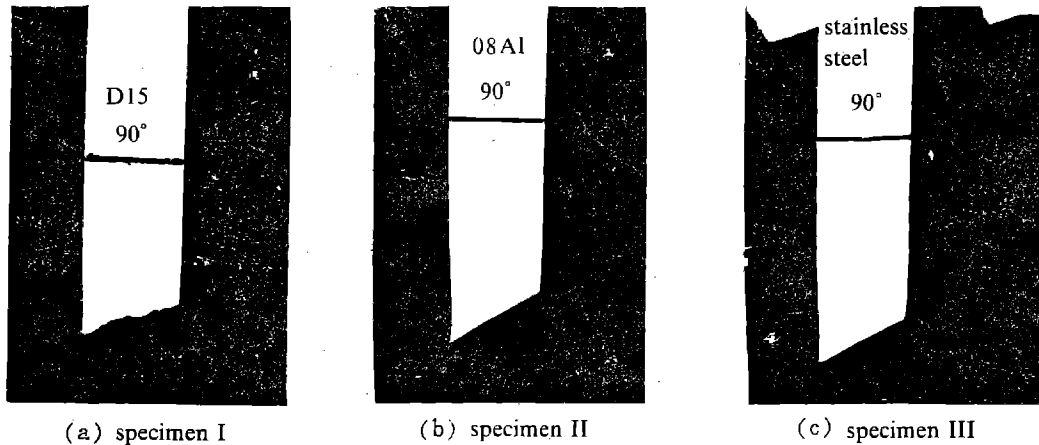


Fig. 2 Fracture configurations of three kinds of specimens

(2) Calculation

In the per-gauging specimens, we take 1/4 of the specimens to calculate, using specimen symmetry. The meshing of initial configuration is shown in Fig. 3. Now, we introduce the B-L non-quadratic yield function describing strong planar anisotropy^[8]

$$f = a|k_1 + k_2|^M + a|k_1 - k_2|^M + c|2k_2|^M - 2\bar{\sigma}^M = 0 \quad (3.1)$$

into updating Lagrange finite element formulation, in which

$$\begin{aligned} k_1 &= \frac{1}{2}(\sigma_{11} + \eta\sigma_{22}), \quad k_2 = \sqrt{\left(\frac{\sigma_{11} - \eta\sigma_{22}}{2}\right)^2 + p^2\sigma_{12}^2} \\ \eta &= \sqrt{R_0(1+R_{90})/[(1+R_0)R_{90}]} \\ a &= 2 - c = 2 - \sqrt{R_0R_{90}/[(1+R_0)(1+R_{90})]} \end{aligned} \quad (3.2)$$

and M is non-quadratic yield function exponent, p is the ratio of the principal stress between biaxial tension and uniaxial tension. From Eq. (3.1), the partial derivative of yield function f to σ_{ij} can be obtained, and then introduced into Eqs. (2.8), (2.9), (2.17) and (2.20), further

into the finite element formulation. In no less generality, $\bar{\varepsilon}^*$ and a_0 in Eq. (2.3) are taken as $0.8n$ and $0.03n$ respectively (n is strain hardening exponent). θ_0 and θ_c in Eq. (2.10) are chosen as 22.5° and 125° , respectively. According to Ref. [8], M value in Eq. (3.1) is taken as 9 for fcc polycrystal, and 6 for bcc one. Loading condition with equal displacement at the end of specimens is carried out. The stretching ratios corresponding to the fracture states of different specimens are determined as the critical condition of calculating termination. Fig. 4 shows the critical fracture configurations. On the left of the 1/4 specimen, effective strain contour distribution is symmetrically plotted. Fig. 5 shows the loading-stretching ratio-necking ratio curves throughout the processes from plastic loading to elastic unloading, in which A_0 is

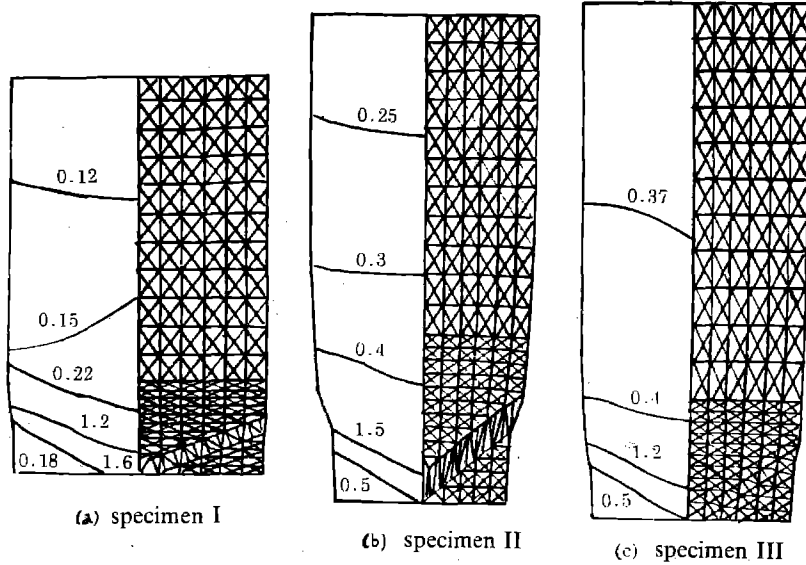
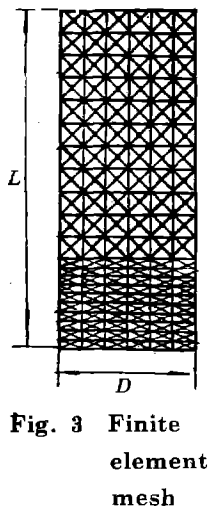


Fig. 4 Fracture configuration of different specimens stretched along 90° rolling direction

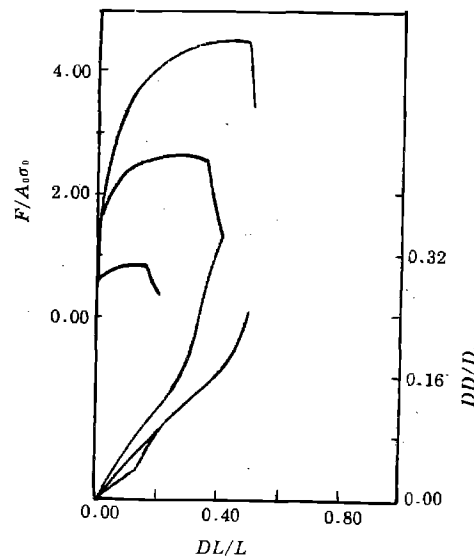


Fig. 5 Loading, unloading-stretching ratio-necking ratio curves

transversal area, σ_0 is initial yield stress, DL is absolute displacement at gauging location, DD is absolute necking amount. From Fig. 5, it can be seen that the necking ratios obtained by calculation is very agreement with experimental ones. Fig. 4 shows that an obvious shear band forms in necking range after unloading occurs. In the shear band, there is obvious high strain distribution, and final fracture location is just along the shear band direction. In addition, the smaller the average anisotropic parameter $R(=(R_0+2R_{45}+R_{90})/4)$ is, the smaller the shear band angle relativizing horizontal direction becomes, which shows the consistence between calculating shear band and experimental fracture direction.

IV. Conclusions

In this paper, a quasi-flow corner theory suitable for large elastic-plastic deformation analysis of anisotropic metals is proposed. This theory realizes not only the smooth transition from flow theory obeying orthogonal law to the corner theory obeying non-orthogonal law, but the continuous transform from plastic loading to elastic unloading. The calculating results of uniaxial tensile instability and strain localization for three kinds of sheet metals show the validity of the present theory.

References

- [1] Keh Chih Hwang, *Non-linear Mechanics of Continuous Media*, Peking University and Tsinghua University Press, (1989), 408–414. (in Chinese)
- [2] S. Stören and J. R. Rice, Localized necking in thin sheet, *J. Mech. Phys. Solids*, 23 (1975), 421–441.
- [3] J. Christofferson and J. W. Hutchinson, A class of phenomenological corner theories of plasticity, *J. Mech. Phys. Solids*, 27 (1979), 465–487.
- [4] M. Gotoh, A class of plastic constitutive equations with vertex effect-I: General theory, *Int. J. Solids Struct.*, 21, 11 (1985), 1101–1116.
- [5] P. Hu, J. Lian and Y. X. Li, Quasi-flow theory of elastic plastic finite deformation, *Acta Mechanica Sinica*, 26, 3 (1994), 275–283.
- [6] P. Hu, Numerical research on localization of plastic flow in plastic and superplastic materials, Ph. D. in Jilin Univ. of Tech., (1993). (in Chinese)
- [7] P. Hu, J. Lian and J. W. Chen, Finite element numerical analysis of sheet metal under uniaxial tension with a new yield criterion, *J. Mater. Proc. Tech.*, 31 (1992), 245–253.
- [8] F. Barlat and J. Lian, Plastic behavior and stretchability of sheet metals, Part I: A yield function for orthogonal sheets under planes stress conditions, *Int. J. Plasticity*, 5 (1989), 51–75.
- [9] J. C. Nagtegaal, D. M. Parks and J. R. Rice, On numerically accurate element solution in the fully plastic range, *Comp. Mech. Eng.*, 4 (1974), 153.